Electronic Supplementary Information

High-voltage honeycomb layered oxide positive electrodes for rechargeable sodium batteries

Chih-Yao Chen,[a] Josef Rizell,[b] Godwill Mbiti Kanyolo, [c] Titus Masese,[*,a,d] Yasmine Sassa,[b] Martin Månsson,[e] Keigo Kubota, [a,d] Kazuhiko Matsumoto, [*a,f] Rika Hagiwara[a,f] and Qiang Xu[*a,d]

[a] AIST-Kyoto University Chemical Energy Materials Open Innovation Laboratory (ChEM-OIL), National Institute of Advanced Industrial Science and Technology (AIST), Sakyo-ku, Kyoto 606-8501, Japan

[b] Department of Physics, Chalmers University of Technology, SE-412 96 Göteborg, Sweden

[c] Department of Engineering Science, The University of Electro-Communications, 1-5-1 Chofugaoka, Chofu, Tokyo 182-8585, Japan

[d] Department of Energy and Environment, Research Institute of Electrochemical Energy (RIECEN), National Institute of Advanced Industrial Science and Technology (AIST), Ikeda, Osaka 563-8577, Japan

[e] Department of Applied Physics, School of Engineering Sciences, KTH Royal Institute of Technology, Roslagstullsbacken 21, SE-106 91 Stockholm, Sweden

[f] Graduate School of Energy Science, Kyoto University, Yoshida, Sakyo-ku, Kyoto 606-8501, Japan

Experimental

Synthesis and material characterization of $Na_2Ni_{2-x}Co_xTeO_6$

Polycrystalline samples of $Na_2Ni_{2-x}Co_xTeO_6$ (x = 0, 0.25 and 0.50) were synthesized through the high-temperature solid-state reaction route. A stoichiometric mixture of TeO_2 (Aldrich, purity of ≥99.0%), NiO (High Purity Chemicals, purity of 99%), CoO (High Purity Chemicals, purity of 99%) and Na_2CO_3 (Rare Metallic, 99.9%)was thoroughly pulverized, pelletized and subsequently calcined at 800 °C for 24 hours in air. Conventional XRD measurements were taken using a D2 Phaser Bruker diffractometer at a Cu-$K\alpha$ wavelength, to confirm the purity and atomic structure of the samples. Structural refinements of $Na_2Ni_{2-x}Co_xTeO_6$ were performed using the Rietveld refinement protocol implemented in the JANA 2006 program and the crystal structure visualization was done using the VESTA software.[1,2] Morphologies of the as-synthesized compounds were analyzed using a scanning electron microscope (JSM-6510LA, JEOL).

Electrochemical measurements

$Na_2Ni_{2-x}Co_xTeO_6$ was mixed with acetylene black (AB) and polyvinylidene fluoride (PVDF) in a weight ratio of 70:25:5. A uniform slurry was prepared by suspending the mixture in *N*-methyl-2-pyrrolidinone, which was then cast onto aluminum foil with a mass loading of 4–6 mg cm^{-2}. The compound was vacuum-dried at 120 °C overnight for complete evaporation of the solvent, punched into composite electrode disks and used as the working electrodes. Metallic sodium discs (Sigma-Aldrich, purity 99.95%) were pressed onto aluminum current collectors were used as the negative (counter) electrodes. An ionic liquid, Na[FSA]–[C_3C_1pyrr][FSA] (FSA: bis(fluorosulfonyl)amide; C_3C_1pyrr: *N*-methyl-*N*-propylpyrrolidinium) with a molar ratio of 2:8 (0.983 M at 25 °C) was used as the electrolyte due to its stable electrochemical properties over a wide temperature range.[3–5] Glass microfiber filters (GF/A, Whatman) vacuum impregnated with the electrolyte were used as the separator. 2032-type coin cells were there after assembled in an Ar-filled glove box and electrochemical measurements were performed using a Bio-Logic SP300 potentiostat or a Hokuto Denko HJ1001SD8 charge–discharge unit. The current density was converted into a

C-rate based on the theoretical capacity of 138.5 mAh g^{-1} necessary for complete Na removal from $Na_2Ni_{2-x}Co_xTeO_6$. The operating temperature (25–75 °C) was controlled by EXPEC thermostat chambers (SU–242 or ST-110).

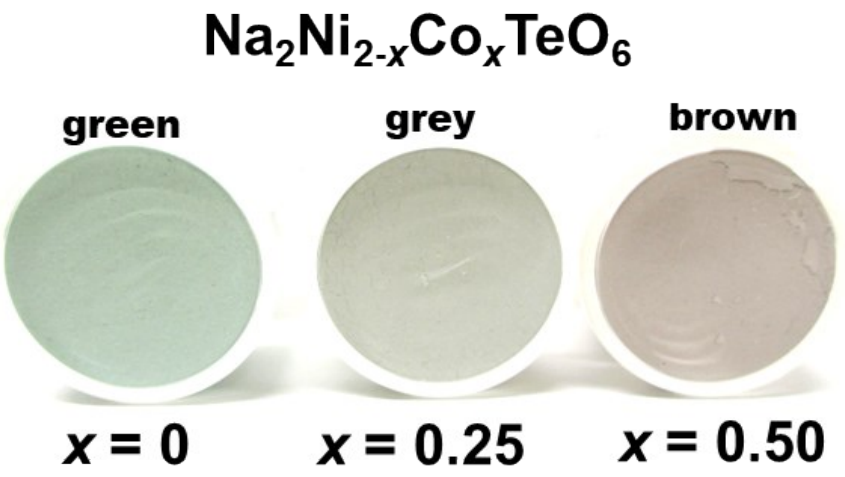

Figure S1. Variation in the color of $Na_2Ni_{2-x}Co_xTeO_6$ (x = 0, 0.25 and 0.50) honeycomb layered oxides, indicating color change with increasing amount of cobalt substitution in $Na_2Ni_2TeO_6$.

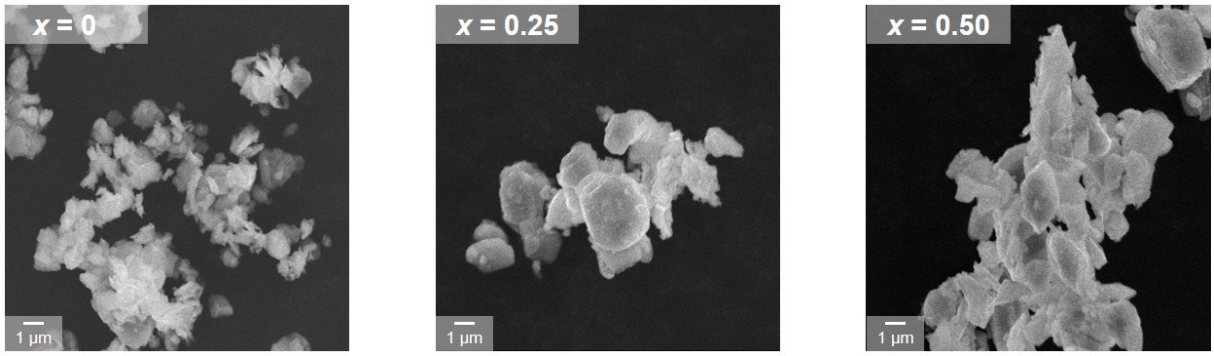

Figure S2. Scanning electron microscopy (SEM) images of the as-synthesized $Na_2Ni_{2-x}Co_xTeO_6$ (x = 0, 0.25 and 0.50) indicating a wide micrometric size particle distribution. Samples appear to have more defined crystalline facets and larger particle sizes than $Na_2Ni_2TeO_6$ upon Co-substitution.

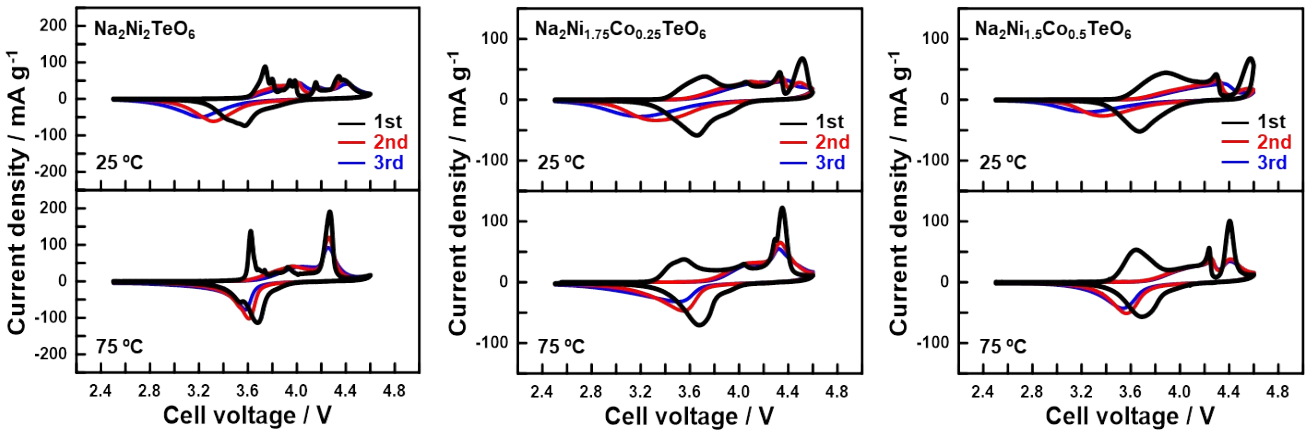

Figure S3. Cyclic voltammograms of $Na_2Ni_{2-x}Co_xTeO_6$ (x = 0, 0.25 and 0.50) electrodes at a scanning rate of 0.1 mV s^{-1} in the voltage range of 2.5–4.6 V. The measurements were taken at 25 °C and 75 °C. A number of redox peaks reminiscent of phase transitions, which tend to be smeared and suppressed upon Co substitution, predominantly occur in the first cycle. Note that different scales have been used for each composition for clarity.

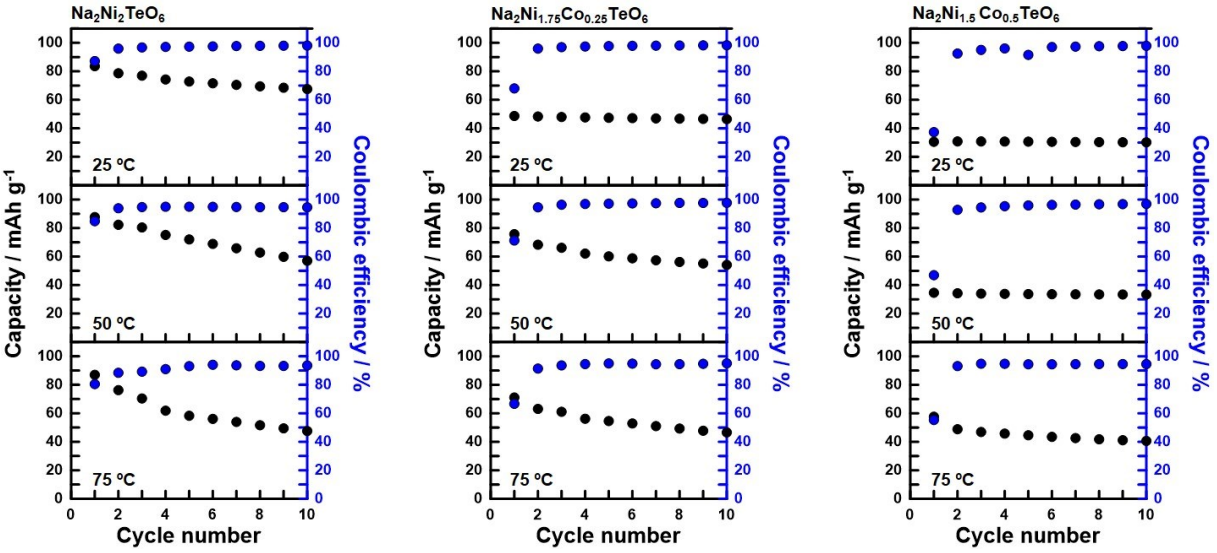

Figure S4. Capacity retention and coulombic efficiency of $Na_2Ni_{2-x}Co_xTeO_6$ (x = 0, 0.25 and 0.50) during galvanostatic (dis)charging at a current density equivalent to 6.925 mA g^{-1} (C/20). The measurements were performed in the voltage range of 2.5–4.35 V and temperature variations of 25 ºC, 50 ºC, and 75 ºC.

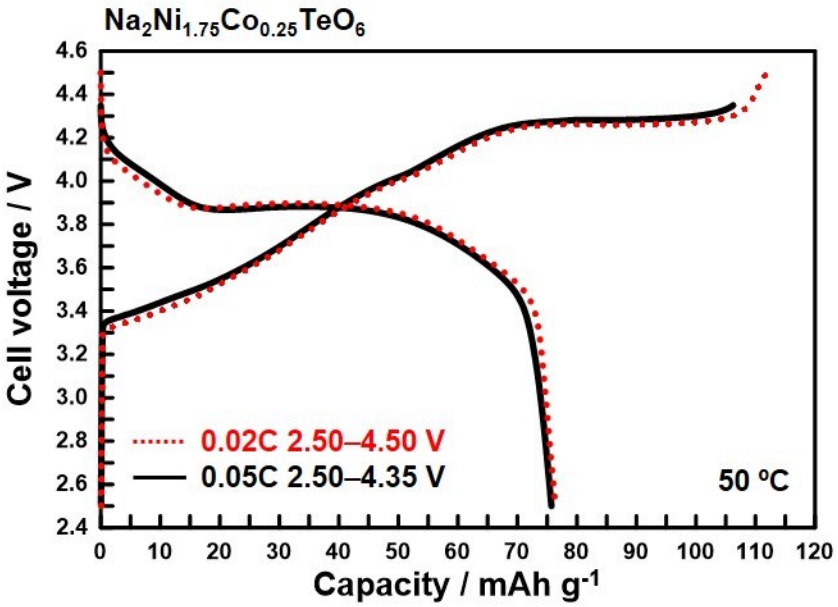

Figure S5. Galvanostatic charge–discharge curves of $Na_2Ni_{1.75}Co_{0.25}TeO_6$ measured at 50 °C for different voltage ranges and current densities. The solid black curves show measurements performed in the 2.5–4.35 V voltage range at a current density of (i) C/20 (6.925 mA g^{-1}). The dotted red curves show measurements performed in the higher cut-off voltage range of 2.5–4.5 V at C/50 (2.77 mA g^{-1}). For both cases, only the first cycle is shown for clarity.

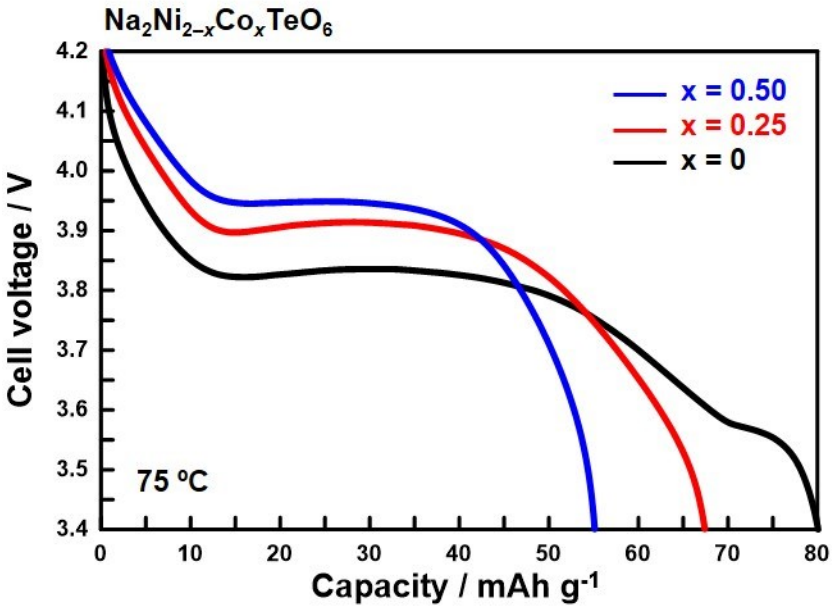

Figure S6. Comparison of the discharge capacity curves of $Na_2Ni_{2-x}Co_xTeO_6$ (x = 0, 0.25 and 0.50) at a current density equivalent to C/20 (6.925 mA g^{-1}) at 75 °C. This figure shows an increase in the average voltage in $Na_2Ni_2TeO_6$ upon partial substitution of Ni with Co, albeit at the expense of the attainable capacity.

Table S1. Atomic coordinates (x, y, z), Wyckoff symbols and occupancies (g) obtained from Rietveld refinement of high-resolution conventional X-ray diffraction data for as-prepared $Na_2Ni_{1.5}Co_{0.5}TeO_6$ (x=0.50 in $Na_2Ni_{2-x}Co_xTeO_6$) indexed in the centrosymmetric space group $P6_3/mcm$ (hexagonal) with lattice constants a = 5.2183(1) Å, c = 11.1449(3) Å, and V = 262.8(1) Å^3. Preferential orientation of (00l) Bragg peaks was treated using the March-Dollase functions.

Atom	Wyckoff	x	y	z	g
Te	2b	0	0	0	1
Co	4d	2/3	1/3	0	0.25
Ni	4d	2/3	1/3	0	0.75
O	12k	0.6445(10)	0.6445(10)	0.5635(5)	1
Na1	6g	0.3565(42)	0	1/4	0.403(5)
Na2	4c	1/3	2/3	1/4	0.184(2)
Na3	2a	0	0	1/4	0.029(9)

R_{wp}=9.57% R_p=6.54% χ^2=2.24

Table S2. Atomic coordinates (*x*, *y*, *z*), Wyckoff symbols and occupancies (*g*) obtained by Rietveld refinement of high-resolution conventional X-ray diffraction data for as-prepared $Na_2Ni_{1.75}Co_{0.25}TeO_6$ (x=0.25 in $Na_2Ni_{2-x}Co_xTeO_6$) indexed in the centrosymmetric space group $P6_3/mcm$ (hexagonal) with lattice constants a = 5.2151(1) Å, c = 11.1514(4) Å, and V = 262.6(1) Å^3. Preferential orientation of (00*l*) Bragg peaks was treated using the March-Dollase functions.

Atom	Wyckoff	*x*	*y*	*z*	*g*
Te	2*b*	0	0	0	1
Co	4*d*	2/3	1/3	0	0.125
Ni	4*d*	2/3	1/3	0	0.875
O	12*k*	0.6517(7)	0.6517(7)	0.5813(3)	1
Na1	6*g*	0.3394(25)	0	1/4	0.401(2)
Na2	4*c*	1/3	2/3	1/4	0.177(5)
Na3	2*a*	0	0	1/4	0.161(3)

R_{wp}=8.51% R_p=6.22% χ^2=2.03

Table S3. Atomic coordinates (x, y, z), Wyckoff symbols and occupancies (g) from Rietveld refinement of high-resolution conventional X-ray diffraction data for as-prepared $Na_2Ni_2TeO_6$ (x=0 in $Na_2Ni_{2-x}Co_xTeO_6$) indexed in the centrosymmetric space group $P6_3/mcm$ (hexagonal) with lattice constants a = 5.2049(1) Å, c = 11.1505(5) Å, and V = 261.6(1) Å^3. Preferential orientation of (00l) Bragg peaks was treated using the March-Dollase functions.

Atom	Wyckoff	x	y	z	g
Te	2b	0	0	0	1
Ni	4d	2/3	1/3	0	1
O	12k	0.6509(7)	0.6509(7)	0.5825(3)	1
Na1	6g	0.3431(24)	0	1/4	0.421(2)
Na2	4c	1/3	2/3	1/4	0.179(3)
Na3	2a	0	0	1/4	0.262(1)

R_{wp}=8.12% R_p=6.00% χ^2=1.95

References

1. V. Petříček, M. Dušek, L. Palatinus, *Z. Kristallogr. Cryst. Mater.* 2014, **229**, 345–352.

2. K. Momma, F. Izumi, *J. Appl. Crystallogr.* 2011, **44**, 1272–1276.

3. K. Matsumoto, Y. Okamoto, T. Nohira and R. Hagiwara, *J. Phys. Chem. C*, 2015, **119**, 7648.

4. C. Y. Chen, T. Kiko, T. Hosokawa, K. Matsumoto, T. Nohira and R. Hagiwara, *J. Power Sources*, 2016, **332**, 51.

5. K. Matsumoto, J. Hwang, K. Kaushik, C. Y. Chen and R. Hagiwara, *Energy Environ. Sci.*, 2019, **12**, 3247.